

Figure 18 Potential energy as a function of separation of fission fragments peak which occurs at a separation of about twice the fission-fragment radius, may still be very far above the energy corresponding to infinite separation. This is illustrated in Figure 18. If the original nucleus is disturbed so that the fragments only separate within certain limits ($r < r_s$) then the nucleus will not undergo fission. If the disturbance is such as to separate the fragments instantaneously by a distance greater than r_s , then fission will result with the fragments going off to infinity. The energy released in that case will be E_f . Thus a trigger energy or excitation energy of E_x can release the fission energy of E_f . For the heaviest nuclei this situation can arise by the capture of a neutron of effectively zero energy. When the neutron is captured the neutron binding energy, which as we have seen is a little less than 8 MeV, then provides this excitation and the full fission energy of about 200 MeV may then be released mainly as kinetic energy of the fission fragments.

5.13 Summary

By appeal to a simple classical model with an empirical overlay of quantum-mechanical effects, the semi-empirical formula arrived at permits, in terms of five adjustable parameters, a description to be given of a mass surface which, with exceptions to be noted in the next chapter, gives a satisfactory fit to the experimental values for many hundreds of nuclei. Using the formula, predictions can be made concerning the stable members to be expected in a set of isobaric nuclei. Criterion of stability against α -decay and spontaneous fission can be arrived at which lead to an explanation of why these processes are limited to particular ranges of A -values. Also some insight is given into the balance of the different contributions to binding energy and into the change in this balance as one proceeds from light to heavy nuclei.

Chapter 6 Nuclear Shell Model

6.1 Introduction

In Chapter 5 the liquid-drop model was developed as a basis for the discussion of a number of nuclear properties, in particular binding energy. This model will again be used in a later chapter to explain further nuclear properties, for example nuclear fission. However, there are certain properties, one of which is the important property of angular momentum, which cannot find a place in any elementary way in the framework of the liquid-drop model. We now proceed to outline a model which developed in parallel with the liquid-drop model and which plays a very important role in certain areas of nuclear physics. We shall see that it depends on assumptions which appear incompatible with those of the liquid-drop model. The reason for these two models, based on apparently contradictory assumptions, each having its areas of useful application, has for long been a central problem in nuclear physics and is a topic to which we return in a later chapter.

6.2 Experimental evidence for 'magic' numbers

Evidence from several different fields of study can be assembled to show that certain values of Z and N , the proton and neutron numbers of a nucleus, confer special properties. These Z - and N -values, which are referred to as the 'magic' numbers, are 2, 8, 20, 28, 50, 82 and 126. We now collect some of the more important strands of the evidence for the existence of these magic numbers.

When the adjustable constants in the semi-empirical mass formula of section 5.5 are chosen for the best general fit to experimentally measured mass values, it is found that the greatest discrepancies are in regions corresponding to magic numbers of protons or neutrons. Whereas the formula reproduces the general trend of the mass surface to an accuracy of 1 or 2 MeV, in the neighbourhood of magic numbers the experimental mass values fall about 10 MeV below the mass-formula values. Thus the indications are that a nucleus with a magic number of neutrons or protons has an unusually large binding energy.

This high binding energy brings in its train several other effects. For example, an examination of the nuclear chart shows that the element with the largest number of isotopes is tin, for which $Z = 50$, while the neutron number corresponding to the greatest number of isotones is $N = 82$.

Estimates of the relative abundance of elements in the universe, based on the chemical analysis of meteorites reaching the earth, on the spectral analysis of solar and stellar bodies, on the spectrum of nuclei in primary cosmic radiation and on studies of the overall composition of the Earth's crust, results in a plot of relative atomic abundance against mass number A , which shows peaks where 50, 82 or 126 nucleons are involved (Alpher and Herman, 1953). There is a very marked peak corresponding to ^{56}Fe which, it is interesting to note, is the end product of the decay of ^{58}Ni which has $Z = N = 28$. Nuclei which, like ^{56}Fe , have a magic number of both neutrons and protons are referred to as *doubly magic*.

Another pointer comes from the field of natural radioactivity. There exist three naturally occurring radioactive series, the thorium series based on the long-lived parent ^{232}Th , the uranium series based on ^{238}U and the actinium series based on ^{235}U . These series terminate in ^{208}Pb , ^{206}Pb and ^{207}Pb respectively, all these terminal nuclides having 82 protons. ^{208}Pb has 126 neutrons in addition, and is therefore doubly magic.

Particularly convincing evidence for 'magic' properties comes from the capture probability for slow neutrons. This is a relatively unlikely process for nuclei having a magic number of neutrons, whereas for nuclei having one neutron less than a magic number it is a highly likely process. For example, neutron capture into the nucleus $^{135}_{54}\text{Xe}$ having 81 neutrons is seven orders of magnitude more likely than capture into $^{136}_{54}\text{Xe}$, which has 82 neutrons. The behaviour of $^{135}_{54}\text{Xe}$ is of great practical importance. It is a fission product of uranium and, with its great appetite for slow neutrons, constitutes a serious source of 'poisoning' in nuclear reactors as it accumulates with operating time.

Nuclei having one neutron more than a magic number also have distinctive properties. They exhibit delayed neutron emission. $^{137}_{54}\text{Xe}$ is one example of this. When it is formed by the β -decay of $^{137}_{53}\text{I}$ it is frequently in an excited state with an energy of excitation higher than the energy of attachment of the least tightly bound neutron. As a result, rather than the excited state decaying to the ground state with the emission of a photon, neutron emission takes place from the excited state. These neutrons are delayed because of their association with the β -decay. ^{137}I is produced in a nuclear reactor as one of the many fission products. It has a half-life of twenty-four seconds. Its presence in the reactor means that when the chain reaction is stopped by, say, the insertion of control rods, the neutron population does not promptly drop to zero. A certain component of this population associated with delayed neutron emitters like ^{137}I falls off with the half-life of these isotopes. This has an important bearing on the problem of adjusting reactor operating levels as it affects the speed of response of the neutron population to the control settings. Another delayed neutron emitter is $^{87}_{36}\text{Kr}$. In this case the phenomenon is associated with the low value of neutron binding in the case of the fifty-first neutron.

The same effects are exhibited if one considers directly the neutron attachment energy. In Figure 19 this quantity is shown on a section of the nuclear chart. It will be observed, by considering the neutron separation energy for each of the chemical elements in the plot, that there is in each case a sharp drop in energy

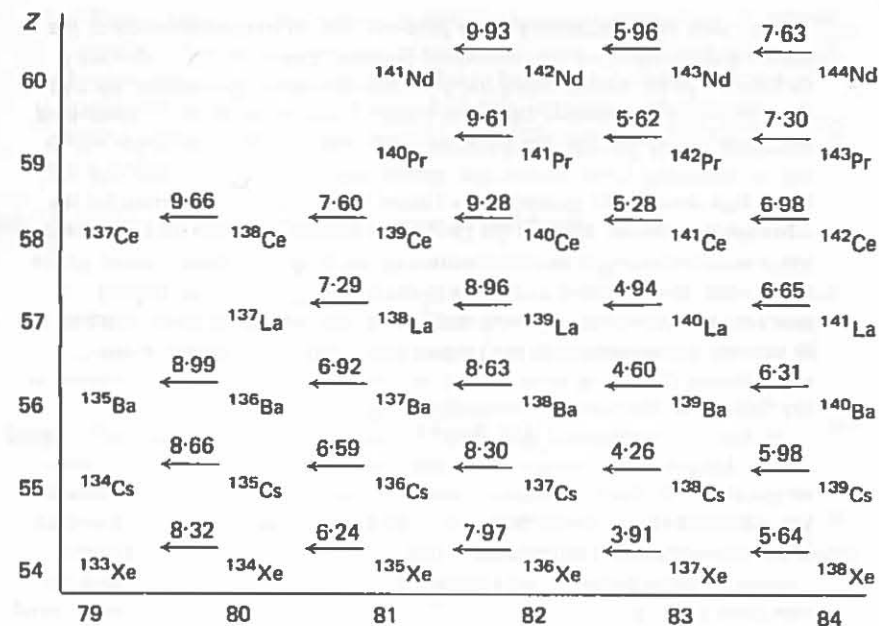


Figure 19 Neutron binding energy is entered to the left of each nuclide to show discontinuity at the magic number, 82, of neutrons in the nucleus

when the eighty-third neutron is reached.

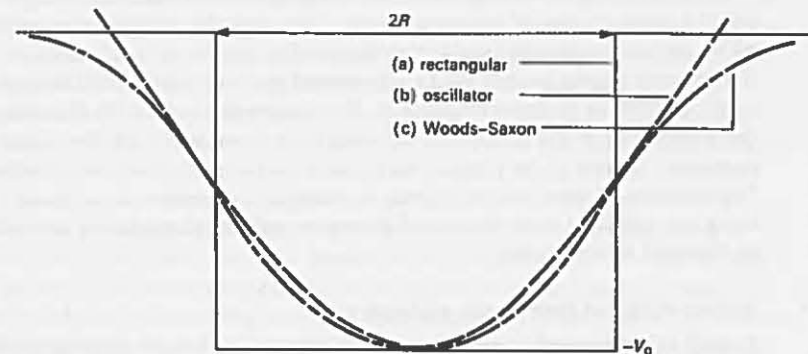
The effects listed to this point all stem from the increased binding energy which a magic number of nucleons confers. There are other effects to be noted which are associated with angular momentum. The pattern of 'spin' values (i.e. intrinsic angular momentum) of the ground states of stable nuclei changes as magic numbers of nucleons are reached. We consider this in detail in discussing the applications of the shell model. It is also to be noted that there are 'islands of isomerism' in areas of the nuclear chart related also to magic numbers of nucleons. The existence of these islands depends on the spin of excited states of nuclei being very different from the ground-state spins and this phenomenon also will be discussed in detail later.

6.3 Nuclear shells and their atomic analogue

Nuclear behaviour with respect to magic numbers of nucleons is reminiscent of the behaviour of atoms with respect to closed shells of electrons. For example, the behaviour of the neutron separation energy as one goes from ^{139}Ce through ^{140}Ce to ^{141}Ce recalls the behaviour of the first ionization energy, which is the measure of the electron separation energy, as one goes from chlorine through argon to potassium. It has become customary to refer to a magic number of nucleons as a closed shell of nucleons in analogy with the electron shells in an atom.

Very soon after Heisenberg's first proposal of a nuclear model based on the proton and the then recently discovered neutron came attempts to develop a shell model of the nucleus using the quantum-mechanical procedures that had been successfully applied to the atom. However, the explanation of closed-shell behaviour arising through the operation of the Pauli exclusion principle, which was so convincing in the atomic case, proved applicable in the nuclear case only to the first three magic numbers. The failure to provide an explanation for the other magic numbers, allied to the resounding success of the liquid-drop model which was developing in parallel, resulted in the temporary abandonment of the shell model. It was revived in 1945 with the discovery that the additional assumption of *spin-orbit coupling* enabled the whole range of magic numbers to be derived. Subsequently the shell model has undergone considerable and sophisticated theoretical development until it now occupies a central position in any theoretical discussion of the nuclear system.

It should be understood that, despite their superficial resemblance with respect to shell behaviour, the nuclear and atomic systems are physically very different. In the atom, the electron motion is dominated by the Coulomb force between the individual electrons and the nucleus; the force between individual electrons is a small perturbation of this main effect. In the nucleus, there is no effect corresponding to the dominant Coulomb force. Each nucleon moves under the combined influence of all the others. The basis of the shell model is that the total effect of all the other nucleons can be represented, in so far as the short-range nuclear interaction is concerned, by a smoothly varying potential having a large negative value in the central region of the nucleus and rising to zero at the nuclear surface. The general features of the shell model should then emerge from a consideration of the motion of a nucleon in this averaged potential.



- (a) $V(r) = 0$ for $r > R$
 $V(r) = -V_0$ for $r < R$
- (b) $V(r) = V_0 \left[\frac{1}{2} \left(\frac{r}{R} \right)^2 - 1 \right]$
- (c) $V(r) = \frac{-V_0}{1 + e^{(r-R)/a}}$ with $a = \frac{R}{5}$

Figure 20 Three different shapes of potential well used in nuclear theory

Various shapes for the nuclear potential considered as a function of distance from the nuclear centre have been suggested and used. We begin by considering the potential to have the shape illustrated in Figure 20(a), that is, constant throughout the nuclear volume rising infinitely steeply to zero at the nuclear surface. The motion of a nucleon in this spherical rectangular potential well will now be investigated.

6.4 The theory of the spherical rectangular potential well

Let the potential well be represented by $V(r)$, where $V(r) = 0$ for $r > R$, and $V(r) = -V_0$, where V_0 is a positive constant, for $r < R$. This well is represented in Figure 20. The wave function of a nucleon in a stationary state in the well must be a solution of the time-independent Schrödinger equation

$$\left[\frac{\partial^2}{\partial x^2} + \frac{\partial^2}{\partial y^2} + \frac{\partial^2}{\partial z^2} \right] \psi + \frac{2M}{\hbar^2} [W - V(r)] \psi = 0, \quad 6.1$$

where M is the nucleon mass and W its total energy. W must have a value such that ψ is zero at the nuclear surface.† ψ is then termed an *eigenfunction*, and W the corresponding *eigenvalue*. Because of the spherical symmetry of the problem, it is convenient to transform to the usual spherical coordinates using the transformations

$$x = r \sin \theta \cos \phi, \quad y = r \sin \theta \sin \phi, \quad z = r \cos \theta.$$

When we change the variables in equation 6.1, it becomes

$$\left[\frac{\partial^2}{\partial r^2} + \frac{2}{r} \frac{\partial}{\partial r} + \frac{1}{r^2} \frac{\partial^2}{\partial \theta^2} + \frac{\cot \theta}{r^2} \frac{\partial}{\partial \theta} + \frac{1}{r^2 \sin^2 \theta} \frac{\partial^2}{\partial \phi^2} \right] \psi + \frac{2M}{\hbar^2} [W - V(r)] \psi = 0. \quad 6.2$$

If the potential is a function of r only, i.e. $V(r)$ does not depend on θ or ϕ , then a separation of the three variables can be achieved. This we develop in two stages. Firstly let

$$\psi(r, \theta, \phi) = R(r) Y(\theta, \phi).$$

Then equation 6.2 may be written

$$Y \frac{d^2 R}{dr^2} + \frac{2Y}{r} \frac{dR}{dr} + \frac{R}{r^2} \frac{\partial^2 Y}{\partial \theta^2} + \frac{\cot \theta}{r^2} R \frac{\partial Y}{\partial \theta} + \frac{R}{r^2 \sin^2 \theta} \frac{\partial^2 Y}{\partial \phi^2} + \frac{2M}{\hbar^2} [W - V(r)] R Y = 0.$$

Multiplying by $r^2/R Y$ and rearranging the terms we have

$$\frac{r^2}{R} \frac{d^2 R}{dr^2} + \frac{2r}{R} \frac{dR}{dr} + \frac{2Mr^2}{\hbar^2} [W - V(r)] = -\frac{1}{Y} \left[\frac{\partial^2 Y}{\partial \theta^2} + \cot \theta \frac{\partial Y}{\partial \theta} + \frac{1}{\sin^2 \theta} \frac{\partial^2 Y}{\partial \phi^2} \right].$$

† This is strictly true only in the limit $V_0 \rightarrow \infty$.

Now the right-hand side depends on θ and ϕ but is independent of r , while the left-hand side depends only on r . It follows that each side must equal a constant independent of r , θ and ϕ . Let this constant be $l(l+1)$ and we then have the two equations

$$\frac{r^2}{R} \frac{d^2 R}{dr^2} + \frac{2r}{R} \frac{dR}{dr} + \frac{2Mr^2}{\hbar^2} [W - V(r)] = l(l+1) \quad 6.3$$

$$\text{and } \frac{1}{Y} \left[\frac{\partial^2 Y}{\partial \theta^2} + \cot \theta \frac{\partial Y}{\partial \theta} + \frac{1}{\sin^2 \theta} \frac{\partial^2 Y}{\partial \phi^2} \right] + l(l+1) = 0 \quad 6.4$$

If it now be assumed that the function Y can be expressed as the product of two functions, one, Θ , a function of θ alone, and a second, Φ , a function of ϕ alone, we can express equation 6.4 as

$$\frac{1}{\Theta \Phi} \left[\Phi \frac{d^2 \Theta}{d\theta^2} + \Phi \cot \theta \frac{d\Theta}{d\theta} + \frac{\Theta}{\sin^2 \theta} \frac{d^2 \Phi}{d\phi^2} \right] + l(l+1) = 0.$$

Multiplying by $\sin^2 \theta$ and rearranging the terms this becomes

$$\sin^2 \theta \left[\frac{1}{\Theta} \frac{d^2 \Theta}{d\theta^2} + \frac{1}{\Theta} \cot \theta \frac{d\Theta}{d\theta} + l(l+1) \right] = -\frac{1}{\Phi} \frac{d^2 \Phi}{d\phi^2}.$$

Each side is seen to be a function of one angular coordinate only, hence again both expressions must equal a constant. Let this constant be m^2 . Therefore

$$\frac{1}{\Phi} \frac{d^2 \Phi}{d\phi^2} = -m^2 \quad 6.5$$

$$\text{and } \frac{1}{\Theta} \frac{d^2 \Theta}{d\theta^2} + \frac{1}{\Theta} \cot \theta \frac{d\Theta}{d\theta} + l(l+1) - \frac{m^2}{\sin^2 \theta} = 0. \quad 6.6$$

We therefore conclude that, assuming the variables to be separable, the original Schrödinger equation 6.2 can be replaced by the three equations 6.3, 6.5 and 6.6, each of these involving only one coordinate. We now proceed to the consideration of the solutions of these equations.

Equation 6.5, involving the azimuthal angle, is the well-known equation for simple oscillations. It has the general solution

$$\Phi(\phi) = A e^{i(m\phi + B)}.$$

In order that this solution be single valued (i.e. $\Phi(\phi) = \Phi(\phi + k2\pi)$, where k is any integer) m must be integral or zero.

Consider now equation 6.6. Let $\mu = \cos \theta$; then in terms of μ this equation can be written

$$(1 - \mu^2) \frac{d^2 \Theta}{d\mu^2} - 2\mu \frac{d\Theta}{d\mu} + \left[l(l+1) - \frac{m^2}{1 - \mu^2} \right] \Theta = 0. \quad 6.7$$

We first consider the special case where $m = 0$ and this equation becomes

$$(1 - \mu^2) \frac{d^2 \Theta}{d\mu^2} - 2\mu \frac{d\Theta}{d\mu} + l(l+1) \Theta = 0. \quad 6.8$$

Solutions for this equation, known as Legendre's equation, may be sought in the form of a power series in μ . In general, there will be two independent solutions. One of these is a series consisting of the odd powers of μ , the other a series

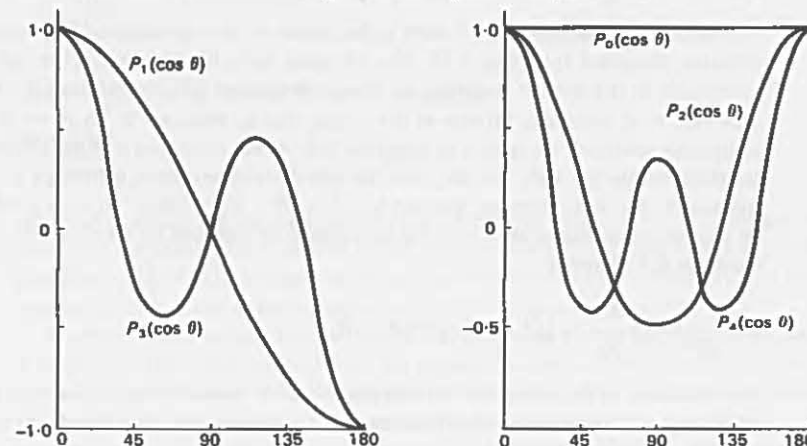


Figure 21 Form of the first few Legendre polynomials

consisting of the even powers. In the general case, no restriction being placed on the value of l , the series do not terminate after a finite number of terms and lead to infinite values of the solution when $\mu = 1$ (i.e. on the z or polar axis). They are therefore not physically acceptable solutions. However, if $l = 0$ or a positive integer, one or other of the series (depending on whether l is even or odd) terminates and leads to a solution which remains finite for the whole range of possible values of μ . These physically acceptable solutions which occur for zero or positive integral values of l are called Legendre polynomials and are denoted by $P_l(\mu)$ or $P_l(\cos \theta)$. As can be shown by finding power-series solutions of equation 6.8, the first few Legendre polynomials are

$$P_0(\cos \theta) = 1, \quad P_1(\cos \theta) = \cos \theta, \quad P_2(\cos \theta) = \frac{1}{2}(3 \cos^2 \theta - 1),$$

$$P_3(\cos \theta) = \frac{1}{2}(5 \cos^3 \theta - 3 \cos \theta), \quad P_4(\cos \theta) = \frac{1}{8}(35 \cos^4 \theta - 30 \cos^2 \theta + 3).$$

Turning now to the case where m is not zero but a positive or negative integer, then, providing $|m| \leq l$, a solution of equation 6.7 which remains finite for all values of μ is

$$P_l^m(\mu) = (1 - \mu^2)^{|m|/2} \frac{d^{|m|}}{d\mu^{|m|}} P_l(\mu).$$

$P_l^m(\mu)$ is called the associated Legendre function.

We now consider the third equation, the radial equation 6.3. We introduce the modified radial wave function $G(r)$ defined by the equation $G(r) = rR(r)$. In terms of G , equation 6.3 can be written

$$\frac{d^2G(r)}{dr^2} + \frac{2M}{\hbar^2} \left[W - V(r) - \frac{l(l+1)\hbar^2}{2Mr^2} \right] G(r) = 0. \quad 6.9$$

This modified radial equation is seen to be similar to the one-dimensional wave equation discussed in section 3.10. The solutions there found however are not acceptable in the present problem, as, when substituted into the relation $R = G/r$, they lead to R becoming infinite at the origin, that is, when $r = 0$. To arrive at acceptable solutions we return to equation 6.3. As the potential is being assumed constant within the well, we can, as in the one-dimensional case, introduce a constant k , the wave number, defined by $k^2 = [W - V(r)] 2M/\hbar^2$. If now $\rho = kr$ be introduced as the variable and the function R be replaced by $\sqrt{(\pi/2kr)} R'$, equation 6.3 becomes

$$\rho^2 \frac{d^2R'}{d\rho^2} + \rho \frac{dR'}{d\rho} + [\rho^2 - (l + \frac{1}{2})^2] R' = 0.$$

This is known as Bessel's equation and the solutions in the theory of functions are known as Bessel functions. Thus, reverting to our original function $R(r)$, a solution can be written as

$$R(r) = \sqrt{\left[\frac{\pi}{2kr} \right]} J_{l+\frac{1}{2}}(kr),$$

where $J_{l+\frac{1}{2}}(kr)$ is the Bessel function of order half an odd integer. The solution can be expressed as

$$R(r) = j_l(kr),$$

$$\text{where } j_l(kr) = \sqrt{\left[\frac{\pi}{2kr} \right]} J_{l+\frac{1}{2}}(kr).$$

$j_l(kr)$ is called the *spherical Bessel function*.

$$j_0(kr) = \frac{1}{kr} \sin kr,$$

$$j_1(kr) = \frac{1}{(kr)^2} \sin kr - \frac{1}{kr} \cos kr.$$

Higher orders can be found by using the recurrence formula

$$j_{l+1}(kr) = \frac{2l+1}{kr} j_l(kr) - j_{l-1}(kr). \quad 6.10$$

6.5 Orbital and magnetic quantum numbers

The formal solutions of the differential equations have been given in some detail to indicate how the restrictions on l and m values arise mathematically. The physical meaning to be assigned to these quantities has now to be discussed.

We note that the expression

$$\frac{l(l+1)\hbar^2}{2Mr^2},$$

which appears in equation 6.9, can be written as

$$\frac{l(l+1)\hbar^2}{2\mathcal{I}},$$

where $\mathcal{I} = Mr^2$ is the moment of inertia of the single nucleon about the origin. In this form the expression is seen to be the rotational kinetic energy of the nucleon providing $\sqrt{l(l+1)}\hbar$ is taken as the angular momentum of the nucleon. For this reason l is termed the angular-momentum or *orbital quantum number*.

If now a particular axis is given physical significance (for example by applying a magnetic field to the system) then the angular-momentum vector $\sqrt{l(l+1)}\hbar$ precesses about the specified direction oriented in such a way that the component of angular momentum along the direction is $m\hbar$, where m is an integer. There are then $2l+1$ different orientations possible, corresponding to the $2l+1$ values of m ranging from $+l$ to $-l$ and including zero. m from the vector model satisfies the same conditions as the separation constant in equation 6.5. It is identified with this separation constant and referred to as the *magnetic quantum number*.

6.6 The radial quantum number

We now consider the radial wave function $R(r)$. We take first the case where $l = 0$. It follows that a solution of 6.3 is

$$R(r) = j_0(kr) = \frac{\sin kr}{kr}.$$

This solution has the required property of remaining finite at the origin, corresponds to a standing wave inside the well and will represent a stationary state if its value is zero at the nuclear boundary. For this condition to be satisfied k must have a value given by

$$\frac{\sin kR}{kR} = 0$$

(in this equation R of course represents the nuclear radius and is not to be confused with the radial wave function). The smallest of the many values of k which satisfy this condition is given by $k_{10} R = \pi$. We note that in this case the wave function has no nodes inside the well. We recall from the definition of k that

$$\frac{\hbar^2 k_{10}^2}{2M} = [W_{10} - V(r)].$$

The potential in the well being constant, $\hbar^2 k_{10}^2/2M$ can be taken as a measure of the energy of the system when the nucleon is in this particular state. We now introduce a radial quantum number ν , numerically equal to one plus the number of radial nodes of the wave function within the nucleus. We use the traditional spectroscopic notation of s, p, d, f, etc. for $l = 0, 1, 2, 3$, etc. and add ν as a prefix to describe the state. In this notation, the case we have been discussing is that of a nucleon occupying a 1s state.

We note that the next highest value of k producing the correct boundary conditions, l still being zero, is given by $k_{20}R = 2\pi$. The wave function will then have one radial node corresponding to $k_{20}r = \pi$ and the radial quantum number will now therefore be equal to two. The state is a 2s state. The argument can obviously be extended to higher ν -values, l of course still being zero.

For $l=1$ we take the next order Bessel function and find $R(r)$ to have the form

$$\frac{\sin kr}{(kr)^2} - \frac{\cos kr}{kr}.$$

The values of k which will produce nodes at the nuclear surface are now given by $\tan kR = kR$. The solutions of this equation can be obtained graphically and are $kR = 4.50, 7.70, 10.9, \dots$. These correspond to the 1p, 2p, 3p, ... states.

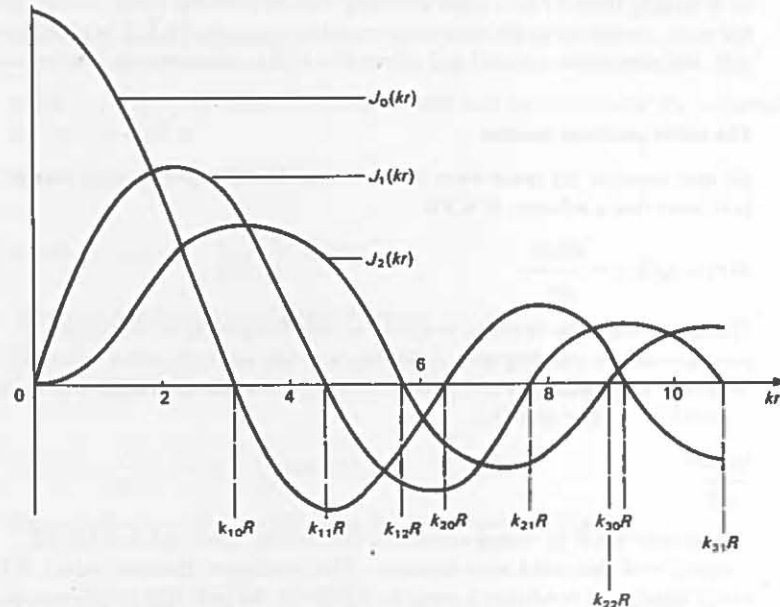


Figure 22 Plot of the first few spherical Bessel functions. The zeros give the $k_{l\nu}R$ values

	$2(2l+1)$	$\Sigma 2(2l+1)$	'magic' numbers
4s	(2)	168	
3d	(10)	166	
2g	(18)	156	
3p	(6)	138	
1i	(26)	132	126
2f	(14)	106	

3s	(2)	92	
1h	(22)	90	82
2d	(10)	68	
1g	(18)	58	50
2p	(6)	40	
1f	(14)	34	28
2s	(2)	20	20
1d	(10)	18	
1p	(6)	8	8
1s	(2)	2	2

Figure 23 Shell-model states for rectangular potential well. The occupation numbers given in the first of the three columns on the right of the diagram are added in the neighbouring column to give the total number of nucleons accommodated up to a given level. The magic numbers above 20 do not find a place in the scheme

The argument can be extended to higher values of l , using higher-order Bessel functions, and kR values can be found corresponding to pairs of radial and orbital quantum numbers. The results for the lower values of these quantum numbers are given in Table 3 and illustrated in Figure 22. In Figure 23 the energies of the states are drawn in the conventional *level diagram*, the associated quantum numbers being indicated at the left-hand side.

Table 3

		s ($l = 0$)				p ($l = 1$)				
ν		1	2	3	4	1	2	3		
$k_M R$		3.14	6.28	9.42	12.57	4.49	7.72	10.90		
		d ($l = 2$)			f ($l = 3$)		g ($l = 4$)		h ($l = 5$) i ($l = 6$)	
ν		1	2	3	1	2	1	2	1	1
$k_M R$		5.76	9.10	12.32	6.98	10.41	8.18	11.71	9.36	10.51

6.7 The number of nucleons in the various shells

It is now postulated that in a given nucleus, having N neutrons, these N neutrons fill the lowest available levels in this scheme. The availability is determined by the Pauli exclusion principle which does not permit two particles to have the same set of four quantum numbers, ν, l, m, m_s , where ν, l and m are as defined in the previous section and m_s is associated with the component of the spin (i.e. intrinsic angular momentum) of the nucleon along a specified direction; m_s has the two values $+\frac{1}{2}$ and $-\frac{1}{2}$. Each level can therefore only contain a limited number of particles. For a given ν and a given l there are $2l + 1$ different possible values of m and two different values of m_s . Thus there are $2(2l + 1)$ different pairs of values of m and m_s available. This quantity is called the occupation number and is shown in brackets to the right of each level in Figure 23. The total number of particles accommodated in the scheme, up to and including a particular level, is indicated to the right of the occupation number of that level in each case. If the magic numbers indeed reflect shell behaviour, then the test of the validity of this level scheme will be the existence of the magic numbers in the last column. It is seen that the first three magic numbers are included but none of the others appear. There are other reasons connected with angular-momentum considerations for believing that this predicted order of levels is not correct.

6.8 Spin-orbit coupling

The suggestion which revitalized the shell model was that a coupling be assumed to exist between the orbital angular momentum and the spin angular momentum of a nucleon. Spin-orbit coupling had been found to be a feature of the atomic system and to play a fundamental and necessary role in determining the details of atomic spectra. In the atom it may be considered to arise from the interaction

of the magnetic dipole moment of the charged, spinning electron with the magnetic field arising from the relative motion of the electron and the charged nucleus. In the nuclear context, however, there is no simple reason for such a coupling to be expected. Its introduction was proposed in a spirit of empiricism.

In the absence of spin-orbit coupling, l and s orient with respect to a specified direction Oz so that the observable components of angular momentum parallel to Oz are $m\hbar$ and $m_s\hbar$. When there is spin-orbit coupling, l and s form a resultant angular momentum j . There are two possible orientations of the spin angular momentum s with respect to the orbital angular momentum l , just as there are two possible orientations of s in an externally applied field. The two orientations give rise to two possible values of j , $j = l + s$ and $j = l - s$. The absolute value of the resultant angular momentum j is $\sqrt{j(j + 1)}\hbar$ and j orients with respect to Oz to give an observable value of angular momentum $m_j\hbar$ parallel to Oz , where m_j is integral or zero, and is less than j , which is half-integral. l and s can be pictured as precessing about j , which in turn, as depicted in Figure 24, precesses about Oz .

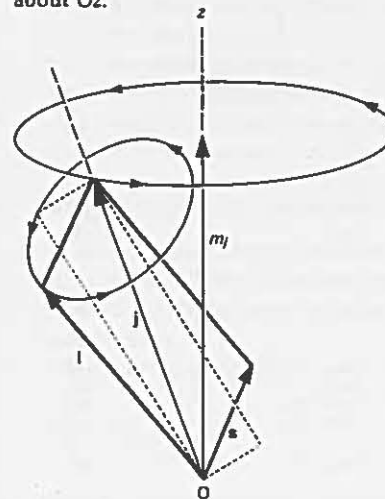


Figure 24 Vector diagram to illustrate the coupling of the orbital angular momentum l with the spin angular moment s to form j with its projection m_j

The four quantum numbers of the nucleon in the absence of spin-orbit coupling are l, s, m_l and m_s . When there is spin-orbit coupling these are replaced by l, s, j and m_j .

We note that there are $2l + 2$ values of m_j associated with the larger of the two j -values (i.e. $j = l + \frac{1}{2}$) ranging from $l + \frac{1}{2}$ to $-(l + \frac{1}{2})$ and $2l$ values of m_j associated with the smaller of the two j -values ranging from $l - \frac{1}{2}$ to $-(l - \frac{1}{2})$, giving $2(2l + 1)$ values in total. This is of course equal to the total obtained by taking the $2l + 1$ values of m_l each in association with two values of m_s . However, spin-orbit coupling implies that the $2l + 2$ states associated with $j + s$ will have a different energy from the $2l$ states associated with $j - s$, whereas in the absence of spin-orbit coupling there is complete degeneracy.

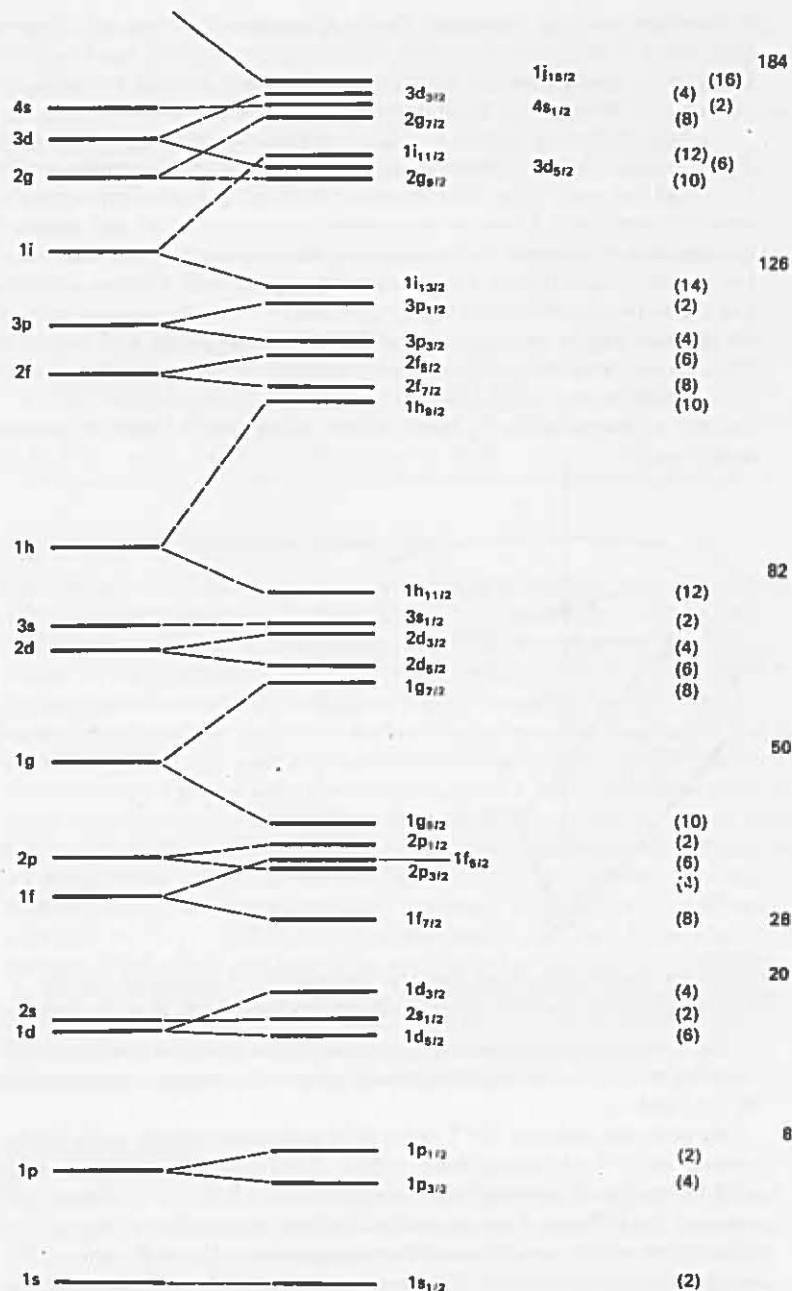


Figure 25 Modifications to the level scheme for a rectangular well brought about by the introduction of spin-orbit coupling. All the magic numbers now find a place and correspond to significantly large gaps between levels

When the hypothesis was first suggested there was no theoretical guidance as to which of the two groups of states had the greater energy or as to the energy difference arising from spin-orbit coupling. The following choice was made on the basis of its leading to a satisfactory level scheme. Firstly, it was assumed that the levels corresponding to $j = l + \frac{1}{2}$ lie lower than those corresponding to $l - \frac{1}{2}$. This is contrary to the behaviour of the electron in the atomic case, where there is a well understood magnetic spin-orbit interaction. Secondly it is assumed that the energy difference between the two sets of levels (i.e. the splitting) is proportional to l . This is in agreement with the results of the atomic system. Figure 25 shows the effect of this spin-orbit splitting on the level scheme. The occupation numbers are shown as before. It is seen now that all of the magic numbers find a place in the last column. Further they can be made to correspond to comparatively large energy gaps in the level scheme and thus to give plausibility to the idea of nucleon shells.

The level scheme in Figure 25 will be valid for nucleons of one kind in a nucleus of given A -value. For any other A -value, the nuclear radius will be different and hence the absolute position of the levels will be altered. The order of the levels however remains unchanged. We have ignored Coulomb effects and hence our result is directly applicable only to neutrons. In the case of protons, the addition of the repulsive Coulomb forces leads to levels which, on an absolute scale, are higher than the neutron levels but are in other respects similar.

6.9 Effect of shape of the nuclear well

We have assumed a highly idealized shape for the nuclear well in the discussion of section 6.4. Other shapes lend themselves to exact mathematical analysis and enable us to see the extent to which the level scheme is dependent on details of nuclear shape.

A potential of the form

$$V(r) = V_0 \left[\frac{1}{2} \left(\frac{r}{R} \right)^2 - 1 \right]$$

corresponds to a harmonic oscillator. Its energy levels are evenly spaced and there are degeneracies which disappear when we go to the other extreme of the rectangular well.

A more realistic intermediate shape has received considerable attention (Woods and Saxon, 1954); the potential shape is given by

$$V(r) = \frac{-V_0}{1 + e^{(r-R)/a}}$$

The shape of this well is compared with the two extremes in Figure 20 and the corresponding energy levels are shown in Figure 26.

We conclude that, although the energy intervals are affected, the order of states (apart from the 1h and 1i states) is not sensitive to the degree of flatness of the well or steepness of the potential rise.

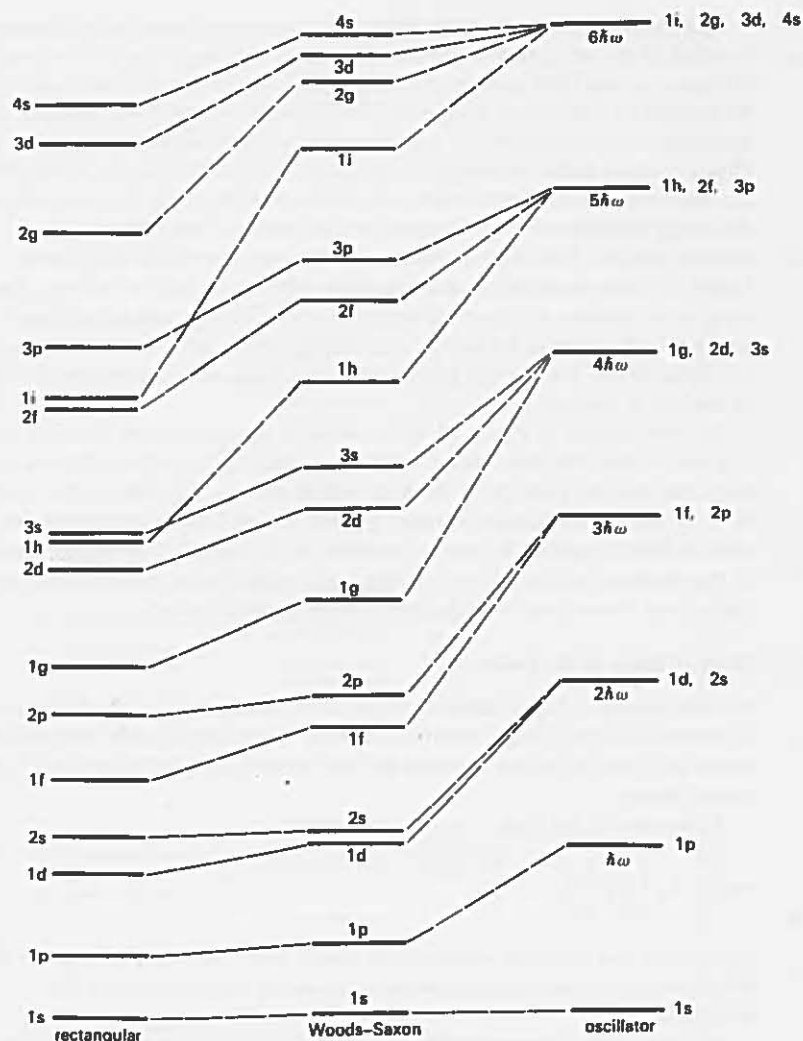


Figure 26 Effect of 'flatness' of well and steepness of sides of well on the level diagram. With the exception of the 1h and 1i states the order of states is not affected

6.10 Nuclear ground-state spins

The shell-model level scheme will now be used to interpret the observed spins (i.e. intrinsic angular momenta) of nuclear ground states.

The nucleons of both kinds will in the ground state (i.e. the state of lowest energy) be in the lowest levels available to them. It is to be expected that when a level is fully occupied the summed contributions of the individual nucleons in the level to the total angular momentum will be zero. When a level is partly filled by an even number of nucleons, it is found experimentally that the nucleons pair off in such a way that the total angular momentum is still zero. We can state this with certainty as there is no exception known to the rule that the measured ground-state spin of an (even, even) nucleus is zero. When the partly filled level contains an odd number of nucleons we assume that again all nucleons, except the last, pair off in a way which leads to cancellation of their contribution to the total spin, and that the spin of the whole nucleus in the ground state is then given by the angular momentum of the single unpaired nucleon. On this assumption we can then predict, from the scheme in Figure 25, the ground-state spin of (odd, even) or (even, odd) nuclei.

For example, $^{25}_{12}\text{Mg}$ will have a spin determined by the thirteenth neutron. This nucleon is seen to be in a $1d_{3/2}$ state and hence the predicted spin value is $\frac{3}{2}$. Again, $^{69}_{31}\text{Ga}$ will have a spin determined by the thirty-first proton. This is seen to be in a $2p_{3/2}$ state and we would thus predict a spin of $\frac{3}{2}$. Predictions made in this way with only a few exceptions (see nuclides marked † in Appendix A) are in agreement with the observed values. The general pattern of spin values provides the angular-momentum evidence for magic numbers mentioned above. For example, as we go from light to heavy nuclei the first time that a spin as high as $\frac{9}{2}$ is encountered is when we reach $^{73}_{32}\text{Ge}$, and we note that the forty-first neutron is the first neutron in the $1g_{7/2}$ level. If we confine attention to (odd, even) nuclei, the first time a spin of $\frac{9}{2}$ is encountered is when $^{93}_{41}\text{Nb}$ is reached, the forty-first proton being the first proton in the $1g_{7/2}$ level.

The direct predictions break down when high spin values are involved. For example, the seventy-first neutron should be the first to occupy the $1h_{11/2}$ level and from there until the eighty-second neutron is reached (even, odd) nuclei would be expected to have spins $\frac{11}{2}$. $^{123}_{52}\text{Te}$ has however a measured spin of $\frac{1}{2}$ as has $^{129}_{54}\text{Xe}$, while $^{131}_{54}\text{Xe}$, $^{135}_{56}\text{Ba}$ and $^{137}_{56}\text{Ba}$ all have spins $\frac{3}{2}$. Attempts to explain this have been made with some success by considering the pairing energy discussed in section 5.5 to be greater the higher the l -values of the two nucleons concerned. If this is correct, then an unpaired nucleon in an h-state would be expected to split a pair of nucleons in an s-state, pairing with one and leaving the other unpaired, providing the difference in the pairing energy for the h- and s-state nucleons exceeds the energy necessary to raise a nucleon from the s to the h energy level.

In the case of (odd, odd) nuclei there will be two unpaired nucleons, one of each kind, to consider. There is nothing in the model to predict how their angular momenta will couple. We saw in section 5.4 that there are only four examples of stable nuclei in this category; in each case the nuclear spin is less than the sum of the j -values of the two unpaired nucleons. This of course must be so whatever the details of the coupling if the behaviour is to be compatible with the shell model. There are one or two examples of unstable nuclei in the (odd, odd) category having long enough half-life to permit determinations of their spins to be made by

experimental methods. The results in these cases too are compatible with compounding of the j -values of the two unpaired nucleons. An interesting case is ${}^{50}_{23}\text{V}$, whose ground state has the high spin value of 4. The twenty-third proton and twenty-seventh neutron are both in $1f_{7/2}$ states and can therefore combine to produce the high value of spin measured.

There are one or two comparatively rare instances of the prediction breaking down among the light nuclei. For example, ${}^{21}_{10}\text{Ne}$ would be expected to have a spin determined by the eleventh neutron, which is in the $1d_{3/2}$ level. Its measured spin is however $\frac{3}{2}$. It has to be conjectured, therefore, that in this case the pairing is broken and the three neutrons in the $d_{3/2}$ level compound their spins to produce a spin of $\frac{3}{2}$.

6.11 Islands of isomerism

Usually, when a nuclear excited state de-excites by the emission of electromagnetic radiation (i.e. γ -ray emission), the transition probability for the process leads to half-lives of the order of 10^{-16} s. We shall see in Chapter 10 that if a very large difference in angular momentum exists between the initial and final states the process can be very much inhibited. In these circumstances the half-life can be very long indeed. For example, there is a state ${}^{110}_{47}\text{Ag}$ which has a half-life for de-excitation of 253 days. When the excited state is long enough lived, the specimen will constitute a γ -source decaying exponentially with time. Apart from the γ -ray there is no other product of de-excitation of the state (see however section 10.2 and Figure 63). The state is said to be an *isomer* and the de-excitation is referred to as an *isomeric transition*. The range of half-lives accessible to experimental measurement has been extended to lower and lower values as electronic techniques have developed. Lives shorter than picoseconds (10^{-12} s) have now been convincingly measured, as we shall discuss in Chapter 10. Although strictly speaking these are isomers as defined above, the term is usually kept for states with a half-life of a microsecond or longer.

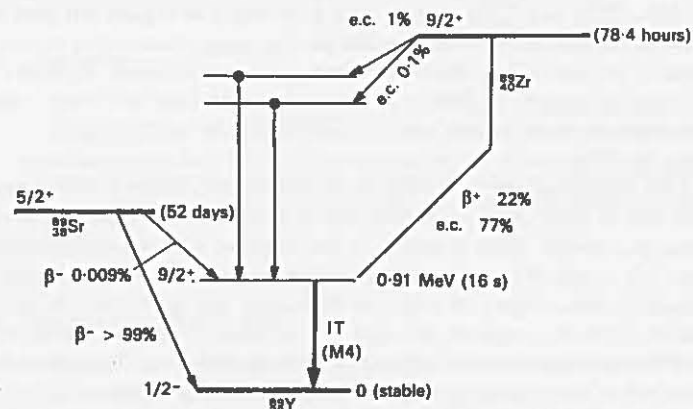


Figure 27 Decay scheme to show the populating and the properties of a $\frac{9}{2}^+$ isomeric state of ${}^{89}\text{Y}$

Within the framework of the shell model, some at least of the excited states of a nucleus can be visualized as arising from a promotion of one nucleon from the topmost level filled, or partly filled, to an unoccupied level of higher energy. Should there be, closely above the topmost occupied level, a level of much higher angular momentum, then the conditions necessary for isomeric behaviour may exist. A good example of this is the stable nucleus ${}^{89}_{39}\text{Y}$. The ground-state spin of this nucleus is dictated by the thirty-ninth proton, which is in the $2p_{1/2}$ state. Close above this is the unoccupied $1g_{7/2}$ state. The promotion of the unpaired proton from the p-state to the g-state gives rise to an excited state of the nucleus, shown in Figure 27, 0.91 MeV above the ground state. The ${}^{89}\text{Y}$ nucleus can be left in this state following the β^- decay of ${}^{89}\text{Sr}$ or the β^+ (or electron-capture) decay of ${}^{89}\text{Zr}$. When so formed the ${}^{89}\text{Y}$ nucleus in decaying to its ground state is involved in a change of $4\hbar$ in angular momentum. As a consequence, the half-life for this electromagnetic transition is observed to be sixteen seconds. A further example of isomeric decay is to be found in the level scheme of ${}^{87}\text{Y}$ illustrated in Figure 28.

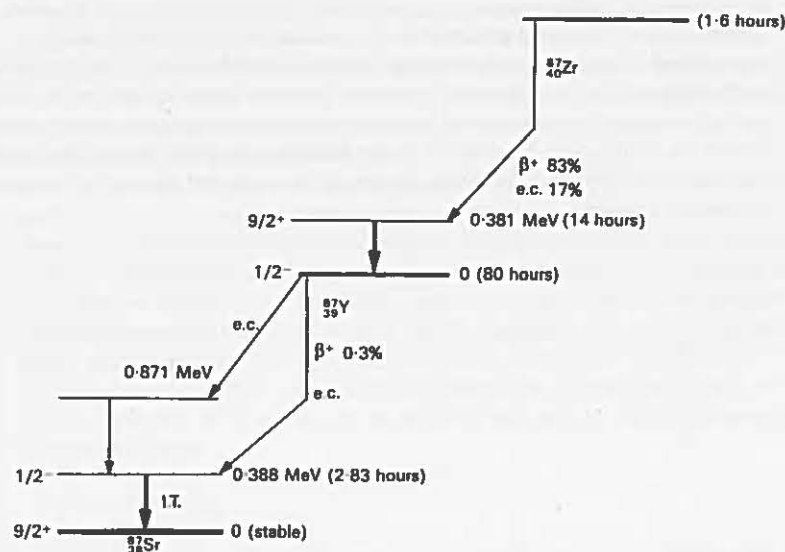


Figure 28 Decay scheme to show the populating and properties of an isomeric state in ${}^{87}\text{Y}$ and an isomeric state in ${}^{87}\text{Sr}$

There is an excited state of the same nature as that found in ${}^{89}\text{Y}$. In this case the excited state lies closer in energy to the ground state, and the half-life (14 hours) as a consequence is even longer. Further, note that ${}^{87}\text{Y}$ decays to yet another isomer, in this case a state of ${}^{87}\text{Sr}$. The ground state of this nucleus has a spin of $\frac{9}{2}$ due to the unpaired forty-ninth neutron. There is a low-lying excited state of spin $\frac{1}{2}$, which can be interpreted as arising from a $2p_{1/2}$ neutron in the state below being